Title

Fluorescence Lifetime Imaging Detects Long-Lifetime Signal Associated with Reduced Pyocyanin at the Surface of Pseudomonas aeruginosa Biofilms and in Cross-Feeding Conditions.

Journal

ACS Infectious Diseases, 11(3)

Authors

Gallagher, Tara
Leemans, Simon
Dvornikov, Alexander
et al.

Publication Date

2025-03-14

DOI

10.1021/acsinfecdis.4c00489

Peer reviewed

ACS Infectious Diseases

pubs.acs.org/journal/aidcbc
Letter

Fluorescence Lifetime Imaging Detects Long-Lifetime Signal Associated with Reduced Pyocyanin at the Surface of *Pseudomonas aeruginosa* Biofilms and in Cross-Feeding Conditions

Tara Gallagher,[#] Simon Leemans,[#] Alexander S. Dvornikov, Kumar Perinbam, Joshua Fong, Christina Kim, Joseph Kapcia, Miki Kagawa, Adam Grosvirt-Dramen, Allon I. Hochbaum, Michelle A. Digman, Enrico Gratton, Albert Siryaporn, and Katrine Whiteson*

Cite This: *ACS Infect. Dis.* 2025, 11, 543−549

Read Online

ACCESS | Metrics & More | Article Recommendations | Supporting Information

ABSTRACT: Understanding bacterial physiology in real-world environments requires noninvasive approaches and is a challenging yet necessary endeavor to effectively treat infectious disease. Bacteria evolve strategies to tolerate chemical gradients associated with infections. The DIVER (Deep Imaging Via Enhanced Recovery) microscope can image autofluorescence and fluorescence lifetime throughout samples with high optical scattering, enabling the study of naturally formed chemical gradients throughout intact biofilms. Using the DIVER, a long fluorescent lifetime signal associated with reduced pyocyanin, a molecule for electron cycling in low oxygen, was detected in low-oxygen conditions at the surface of *Pseudomonas aeruginosa* biofilms and in the presence of fermentation metabolites from *Rothia mucilaginosa*, which cocolonizes infected airways with *P. aeruginosa*. These findings underscore the utility of the DIVER microscope and fluorescent lifetime for noninvasive studies of bacterial physiology within complex environments, which could inform on more effective strategies for managing chronic infection.

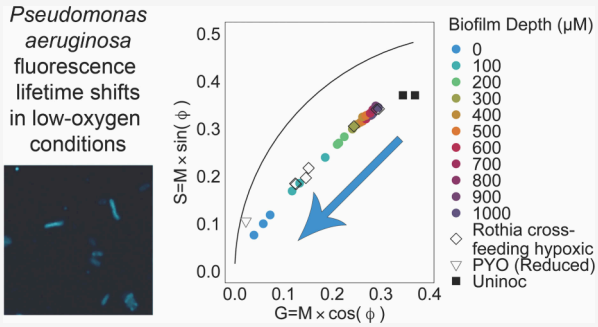

KEYWORDS: *Fluorescence, fluorescence lifetime, biofilm, Pseudomonas aeruginosa, pyocyanin, phenazines*

Biofilms are microbial communities characterized by steep chemical gradients, such as oxygen and nutrient concentrations.[1−4] Understanding bacterial physiology in chemical gradients is critical to improving treatment of biofilm-associated infections, including those found in chronic wounds and Cystic Fibrosis (CF) airways. However, characterizing oxygen gradients in biofilms is challenging due to the difficulty of preserving the integrity of the complex chemical environment while resolving depth-dependent signals in optically scattering samples.

Pseudomonas aeruginosa is one such opportunistic pathogen that must survive in oxygen gradients common in biofilms. *P. aeruginosa* survives in low oxygen through anaerobic respiration via denitrification[5,6] and secreting phenazines,[7,8] which are colorful, electron-recycling molecules that also contribute to disease progression and antibiotic tolerance.[7−11] Low oxygen along with high cell density[12,13] and fermentation metabolites[14,15] promote production of the phenazine pyocyanin. Pyocyanin can be retained in biofilms by extracellular DNA,[16] allowing electron cycling across biofilms.

Given its role in hypoxic survival and disease, detecting pyocyanin in biofilms is of interest. Pyocyanin is a blue-pigmented, nonfluorescent molecule in its oxidized form.[10,17] The reduced form of pyocyanin is fluorescent, with an emission spectra that overlaps with NADH and pyoverdine.[18] Hyperspectral imaging can unmix multiple fluorophores,[18] though commercial microscopes have limitations in imaging depth-dependent signals. The DIVER (Deep Imaging Via Enhanced Recovery)[19,20] is a custom-made microscope that measures fluorescent intensity and fluorescent lifetime throughout highly scattered samples.

Fluorescent lifetime refers to the exponential decay of the fluorescence intensity and can be used to identify multiple fluorophores contributing to a signal. Fluorescent lifetime imaging microscopy (FLIM) data can be represented using phasors, a fit-free approach to analyze FLIM data.[21] The FLIM-phasor represents longer lifetimes at the origin ($G = 0$, $S = 0$), and shorter lifetimes near the right corner ($G = 0$, $S = 1$) (Figure 1). Fluorophores with single exponential decays appear

Received: June 13, 2024
Revised: January 25, 2025
Accepted: February 6, 2025
Published: March 4, 2025

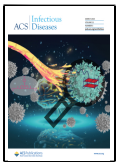

https://doi.org/10.1021/acsinfecdis.4c00489
ACS Infect. Dis. 2025, 11, 543−549

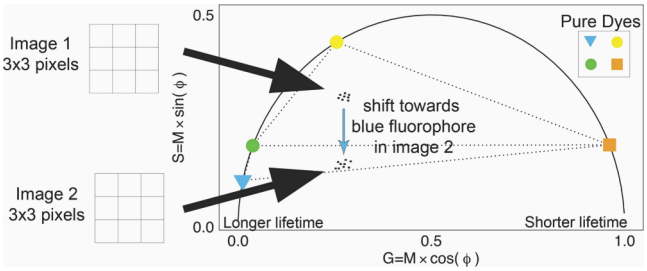

Figure 1. Example of the FLIM phasor approach. The phasor G (x axis) and S (y axis) coordinates represent the cosine and sine components of the Fourier transform of a fluorescent decay trace.[21] Species closer to the origin of the phasor have long lifetimes. Monoexponential fluorescent species land on the "universal circle". The four colored shapes represent pure fluorophore dyes. Shifts in the phasor signal are indicative of changes in the relative abundance of the species. In the example, the biological system consists of four species, and the blue triangle occupies a region in the phasor not shared by the other dyes. The system shifts toward the blue triangle in "Image 2".

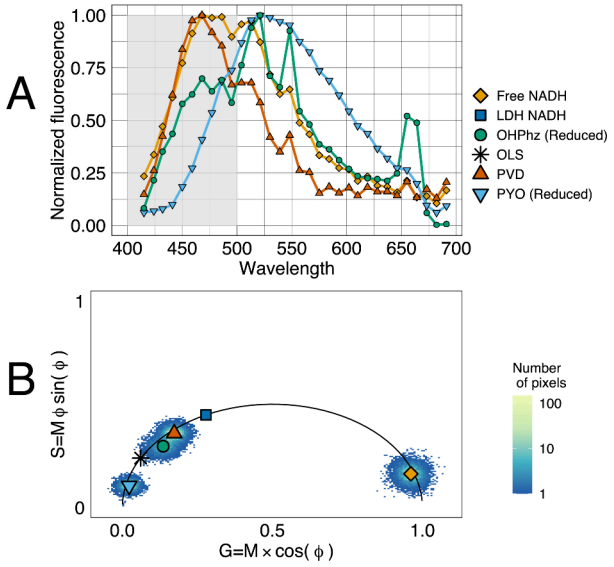

Figure 2. Fluorescent spectra and lifetime phasor of some of the fluorescent metabolites produced by *P. aeruginosa* (two-photon excitation of 740 nm). (A) Fluorescence emission spectra normalized by maximum peak intensity of fluorophores which emit in the 400−500 nm window (gray-shaded box). (B) FLIM-phasor of pure solutions collected with blue emission filters (400−500 nm). Points represent phasor G and S coordinates from a fluorescence lifetime image, colored by the number of pixels. The large shapes represent the mean G and S values for each fluorescent solution. The mean G and S values for LDH NADH and OLS were determined from previously reported fluorescence lifetimes.[23,25]

on the "universal circle" of the phasor (Figure 1). Samples containing multiple fluorophores will generate a phasor signal within the area formed. The signal's distance from each contributor can be used to calculate relative contributions, though there are limitations. Specifically, for single-measurement imaging approaches (e.g., first-harmonic FLIM) also used in this study, a maximum of two or three species can be unmixed.[21,22] In complex systems with more than three species, the phasor can still be used to track physiological changes, particularly when the fluorophore of interest has a distinct "phasor window" or occupies a region of the phasor space that is not shared by other fluorophores (Figure 1)[23]

Results and Discussion. *Spectral and FLIM Characterization of P. aeruginosa Fluorophores.* The 2-photon emission spectra of eight fluorophores were characterized with a hyperspectral imaging microscope (740 nm excitation and emission range of 400−690 nm). The fluorophores included ubiquitous metabolites, such as coproporphyrin, flavin adenine dinucleotide, and nicotinamide adenine dinucleotide, in addition to pyoverdine and phenazines, 1-hydroxyphenazine, phenazine-1-carboxylic acid, phenazine-1-carboxamide, and pyocyanin (Figure S1). Chemically and electrochemically reduced pyocyanin had a peak emission at 520 nm (Figure S2, Figure 2A). The peak emission at 520 nm differed from a previous study, which found chemically reduced pyocyanin had a peak at 475 nm, despite using identical reduction methods and similar fluorescent approaches.[18]

Based on spectral analyses (Figures 2A and S1), four of the eight fluorophores (NADH, reduced pyocyanin, reduced 1-hydroxy-phenazine, and pyoverdine) can be captured by the FLIM acquisition parameters used in downstream experiments, which included a blue emission filter (400−500 nm). While the spectrum of the pyocyanin precursor 5-methyl phenazine-1-carboxylic acid was not measured in this study due to commercial unavailability, previous studies have reported an emission peak at 620 nm.[18,24] The fluorescence of 5-methyl phenazine-1-carboxylic acid would likely contribute minimally to the signal detected by the blue emission filter.

The FLIM-phasor positions of solutions of free NADH, reduced 1-hydroxyphenazine, reduced pyocyanin, and pyoverdine are on the universal circle, suggesting that the signals originate from a single exponential decay (Figure 2B). For reference, also depicted are the previously reported phasor coordinates of lactate dehydrogenase (LDH) bound NADH[26] and an oxidized lipid signal (OLS).[23] Notably, reduced pyocyanin had a long lifetime signal of >10 ns, occupying a region in the phasor not shared with other fluorophores from G = 0.02, S = 0.1 to G = 0.06, S = 0.2(Figure 2B).

The emission spectra and lifetime of pyocyanin shifted with increasing TCEP concentrations, indicative of a longer fluorescence lifetime as the solution was further reduced (Figure S2). Pyocyanin was nearly on the FLIM universal circle when mixed with a 1:1 ratio of TCEP in an anaerobic chamber (Figures 2B and S2B).

Longer Fluorescence Lifetimes at the Surface of P. aeruginosa Biofilms When Limiting Oxygen Exposure. To recapitulate slower bacterial growth observed in infections,[27,28] colony biofilms were grown for 72 h in soft agar. The radial center of the colony, or inoculation point, was imaged axially using the DIVER microscope to capture signals associated with biofilm depth in the oldest population.[19,20] Laser power was increased with imaging depth to compensate for signal attenuation (Figure S3A,B). Prolonged laser exposure did not significantly affect fluorescence lifetime signals, as the phasor coordinates were similar when comparing the first frame to all frames for a given sample (Figure S3C), where a higher number of acquired frames had lower noise (Figure S3D).

Two strains were cultured: wild-type (WT) and a phenazine double mutant *P. aeruginosa* PA14 Δ*phzA1-G1*/Δ*phzA2-G2* (Δ*phz*). The phasor position of *P. aeruginosa* cultures was distinct from that of uninoculated media, except for Δ*phz* strains grown in ASM, likely due to high amounts of NADH in ASM (Figure S4, Figure 3B,C). The FLIM-phasor signal of the

https://doi.org/10.1021/acsinfecdis.4c00489
ACS Infect. Dis. 2025, 11, 543−549

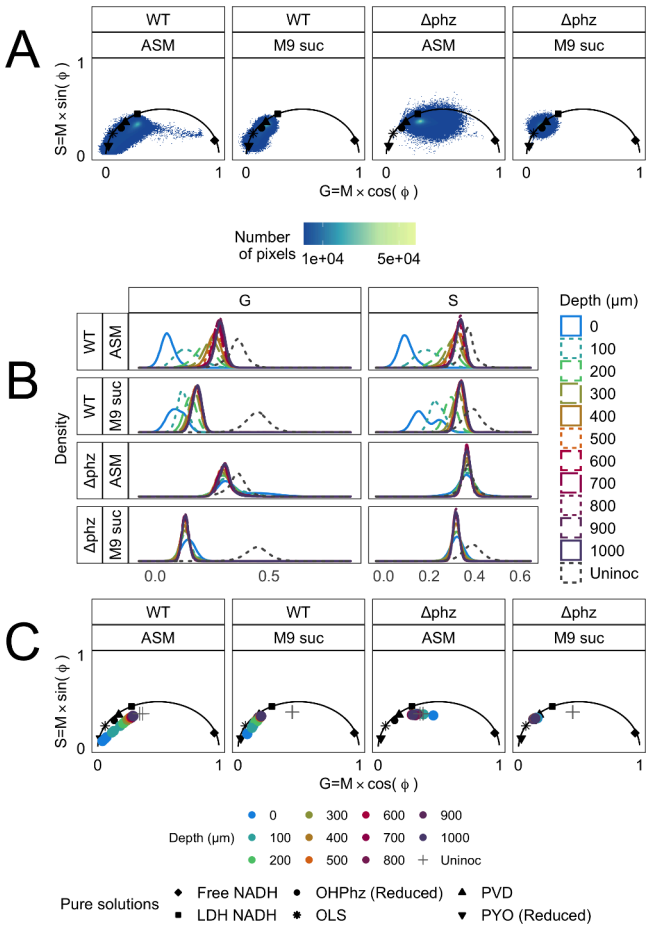

Figure 3. Fluorescence lifetime at different depths of *P. aeruginosa* PA14 biofilms. (A) Fluorescence lifetime phasor of *P. aeruginosa* PA14 WT and Δ*phz* strains (*P. aeruginosa* PA14 Δ*phzA1-G1*/Δ*phzA2-G2*) grown in ASM or M9 succinate soft agar. Biofilms were imaged at 100 μm intervals from the biofilm surface (0 μm) to 1000 μm deep, with three replicates per strain and media type (132 images in total). The fluorescence lifetime phasor of each image was plotted as *G* and *S* values, with the color indicating the pixel quantity. Mean *G* and *S* values of fluorescent solutions from Figure 1 are displayed as black shapes. (B) The one-dimensional distributions of phasor *G* and *S* values showed a significant leftward shift in the WT biofilms compared to Δ*phz* (Wilcoxon rank sum test, *p*-value <0.05). Line type and color are indicative of biofilm depth. The gray dotted line is the uninoculated M9 succinate or ASM media (2 images). (C) Mean *G* and *S* values for each image, colored by biofilm depth. The gray crosses represent mean *G* and *S* values for uninoculated ASM and M9 succinate. The mean *G* and *S* values for WT PA14 were significantly different at the biofilm surface than at other measured depths (200−1000 μm for M9 succinate and 100−1000 μm for ASM; Table S1).

WT strains shifted with biofilm depth in both ASM and M9 succinate, as demonstrated by a shift in the *G* and *S* distributions (Figure 3A,B). The mean *G* and *S* values also had a depth-dependent shift for the WT strain (Figure 3C; Table S1). Specifically, WT PA14 had significantly different phasor *G* and *S* values at the surface of the biofilm compared to measurements at deeper layers in ASM and M9 succinate (*t* test, FDR < 0.05; Table S1). The depth-dependent lifetime shift was not observed in the Δ*phz* cultures (Figure 3, Table S1). The surface of the WT biofilm was dominated by a longer lifetime species. The long fluorescent lifetime signal associated with the WT *P. aeruginosa* cultures was *not* observed in other microbial genera (Figure S5) and has been reported in previous FLIM studies.[29,30] Examples of fluorescent intensity images (Figure 4A) with the FLIM-phasor signal color-mapped

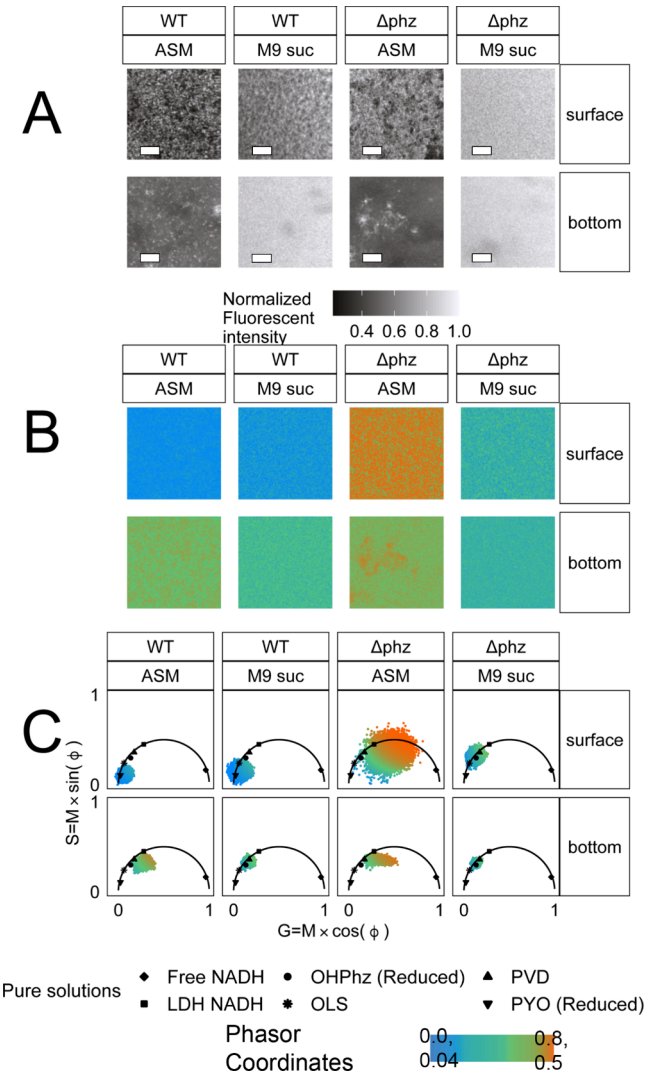

Figure 4. Fluorescence intensity and lifetime images at the surface and 300−1000 μm deep into *P. aeruginosa* PA14 biofilms. (A) Autofluorescent intensity images of *P. aeruginosa* PA14 WT and Δ*phz* strains grown in ASM or M9 succinate soft agar. Scale bar = 20 μm. (B) Fluorescence lifetime images at the surface and 300−1000 μm deep into *P. aeruginosa* biofilms. In (B), each pixel in the image is colored based on phasor position from (C). For reference, mean *G* and *S* values of pure fluorescent solutions from Figure 2 are displayed as black shapes (C). The same color map was used for all lifetime images, where blue is indicative of a longer lifetime near the origin of the phasor.

on top of the image (Figure 4B,C) suggest that secreted molecules contributed to the signal both inside and outside of the cell clusters.

Given that other phenazines emit a low fluorescent signal within the emission filter range and reduced 1-hydroxyphenazine has a short fluorescence lifetime distinct from reduced pyocyanin (Figures 2 and S1), reduced pyocyanin likely produces the long lifetime signal found at the surface of WT *P. aeruginosa* biofilms (Figures 3 and 4).

We initially hypothesized there would be higher levels of reduced pyocyanin deeper in the biofilm[7−9] due to less oxygen

https://doi.org/10.1021/acsinfecdis.4c00489
ACS Infect. Dis. 2025, 11, 543−549

exposure. However, the long lifetime signal associated with reduced pyocyanin was prominent at the biofilm surface. Specifically, the reduced pyocyanin signal was prominent after the addition of a coverslip to the biofilm surface (Figure S6), where there was high density of *P. aeruginosa* growth (Figures 3 and 4). This model agrees with previous observations that population density controls phenazine biosynthesis[12,13] and oxygen is required for pyocyanin biosynthesis.[31] Although it may seem counterintuitive, pyocyanin has the highest affinity for oxygen out of other studied phenazines,[32] and in locally anoxic conditions, *P. aeruginosa* couples pyocyanin reduction with oxidation of glucose and pyruvate.[33] Reduced pyocyanin is secreted and oxidized extracellularly,[8,9] and a portion of pyocyanin is retained in the biofilms when bound to extracellular DNA to enable electron cycling across biofilms.[16]

P. aeruginosa Fluorescence Lifetime Shifts in the Presence of Rothia Metabolites. Although incapable of anaerobic fermentation, *P. aeruginosa* cocolonizes infection sites with fermenting microbes, including *Rothia mucilaginosa*. To explore the effect of fermentation metabolites on *P. aeruginosa* FLIM signal, *P. aeruginosa* PaFLR01 was grown planktonically with supernatant from *R. mucilaginosa* (M9 suc + sup), in M9 media alone (M9 suc), or in ASM (the background media of the *Rothia* supernatant) (Figure 5). The FLIM *G* and *S* measurements had wide distributions (Figure 5A,B), contributing to the noisy spotted patterns in the FLIM images (Figure 5D). Still, the *S* distribution of *P. aeruginosa* grown in M9 suc + sup was significantly shifted to the left toward reduced pyocyanin relative to the ASM and M9 suc controls (Figure 5A,B), and the mean phasor values of M9 suc + sup relative to ASM were significant or nearly significant (*G* coordinate FDR < 0.05; *S* coordinate FDR = 0.1; Figure 5B, Table S2). Similar to the WT biofilm cultures (Figure 4B), the FLIM signal was similar within and across cells when the phasor signal was color-mapped back onto the images (Figure 5C,D). Although distinct FLIM signatures correlated with bacterial cells in some cases (such as the bright orange objects in the M9 succinate image in Figure 5D), the FLIM signal was spatially homogeneous for the most part, indicating the contribution of secreted molecules to the signal. Previous studies showed that *P. aeruginosa* metabolizes pyruvate and lactate generated by *R. mucilaginosa* in the supernatant.[34] The presence of fermentation metabolites may be used as an indicator of low oxygen, driving the production of pyocyanin before oxygen depletion.

Conclusion. The present study demonstrates the spatial mapping of metabolites throughout an intact *P. aeruginosa* biofilm. We detected a long fluorescent lifetime signal associated with reduced pyocyanin at the surface of intact biofilms and in the presence of fermentation metabolites. Given the significance of pyocyanin in disease progression and *P. aeruginosa* physiology, the DIVER FLIM approach shows promise as a tool to advance the understanding of infections and treatment strategies in infection-relevant models.

Limitations and Future Directions. Due to the large number of detected fluorophores, calculating the relative abundance of each species was not possible. In this study, any fluorescent lifetime shifts beyond the reported 7.8 ns oxidized lipid signal[23] were assumed to be reduced pyocyanin, which exhibited a longer lifetime signal (>10 ns). However, since oxidized pyocyanin is nonfluorescent, we could not determine whether shifts in the fluorescent signal toward reduced pyocyanin resulted from the reduction of an existing pool or the synthesis of additional pyocyanin. Combining FLIM with hyperspectral approaches and conducting experiments under

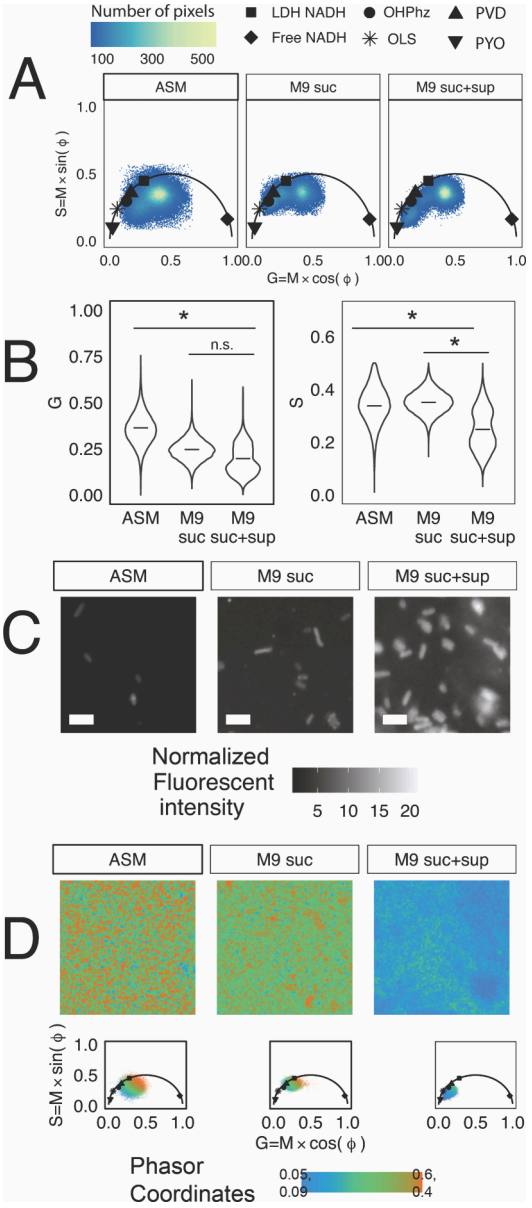

Figure 5. *P. aeruginosa* PaFLR01 fluorescence lifetime shifts when cross-fed with *Rothia* supernatant. (A) Fluorescence lifetime phasor of PaFLR01 grown in three media types under hypoxic conditions. Scatter plot points are *G* and *S* coordinates of pixels from fluorescence lifetime images of PaFLR01 grown in hypoxic ASM (14 images), M9 suc (8 images), or M9 suc + sup (7 images). Mean *G* and *S* values of pure fluorescent solutions are displayed on the universal circle as black shapes. The two-dimensional *G* and *S* distributions were significantly different for each pairwise comparison (ASM vs M9 suc, ASM vs M9 suc + sup, M9 suc vs M9 suc + sup; Fasano-Francheschini Test, *p*-value <0.05). (B) The one-dimensional distributions of *G* and *S* for each media condition; the middle bar is the mean *G* and *S* of all images. M9 suc + sup S distributions were significantly lower than the M9 suc and ASM conditions (*p*-value <0.05, Table S2). (C) Examples of fluorescent intensity images from the cross-feeding experiment. Scale bar = 3 μm. (D) The fluorescence lifetime image (top) from three samples, colored by the phasor position (bottom). Blue is indicative of a longer lifetime near the origin of the phasor.

https://doi.org/10.1021/acsinfecdis.4c00489
ACS Infect. Dis. 2025, 11, 543−549

more controlled redox conditions shows promise for disentangling metabolic shifts in these complex systems.[35]

METHODS

Chemicals and Bacterial Media. Ten millimolar stocks of pyocyanin (Sigma-Aldrich P0046) and 1-hydroxyphenazine (OHPhz) (Fisher H0289100MG) were dissolved in 20% ethanol and methanol, respectively. Phenazine-1-carboxamide (PCN) (Sigma-Aldrich AMBH2D6F8130) and phenazine-1-carboxylic acid (PCA) (Fisher 2538-68-3) were dissolved in chloroform to 4.5 mM. Dissolved phenazine stocks were stored at −20 °C.

Artificial sputum and M9 minimal media with 40 mM succinate soft agar in large Petri dishes (150 × 15 mm) were used to grow *P. aeruginosa* biofilms. Both media recipes were modified from Gao et al.[34] to include 0.28% final agar concentration.

Bacterial Strains and Growth. *P. aeruginosa* PA14 and phenazine knockout *phzA1-G1/A2-G2* were obtained from Dianne Newman (California Institute of Technology). For biofilm imaging, the bacteria were grown overnight on Todd-Hewitt agar, and individual colonies were inoculated into the center of the artificial sputum (ASM) or M9 succinate soft agar plates.[34] The biofilms were grown in an aerobic incubator at 37 °C for 3 days.

For the cross-feeding experiment, *Rothia mucilaginosa* RmFLR01[14,34] was grown in liquid (ASM) for 48 h. *Rothia*-derived supernatant was then filtered and cross-fed to a cystic fibrosis isolate, *P. aeruginosa* FLR01, in liquid M9 succinate for 72 h in hypoxic conditions (2% oxygen). For the control, *P. aeruginosa* FLR01 was also grown in liquid M9 succinate media or ASM alone. After the 72 h incubation, 5 μL of the *P. aeruginosa* FLR01 culture was transferred to a slide and mixed with 5 μL of 1% prewarmed agar, heated to approximately 55 °C in a hypoxic chamber (2% oxygen). To maintain a hypoxic environment, the coverslip was then sealed onto the slide with nail polish. The slide was removed from the chamber and imaged within 30 min.

Chemical and Electrochemical Reduction of Phenazines. Prior to reduction, dissolved phenazine stocks were moved from −20 °C to a Coy Anaerobic Chamber (0% oxygen).

For chemical reduction of pyocyanin, 75 to 600 μM stocks of pyocyanin were diluted in 1× MOPS buffer with TCEP concentrations ranging from 0.1 to 125 mM (pH 7).

For electrochemical reduction, a fresh stock of 821 μM of pyocyanin was prepared in ammonium acetate 0.1 M KCl MOPS buffer and electrochemically reduced following Wang and Newman.[32] The electrochemical cell consisted of a glassy carbon working electrode, a platinum wire counter electrode, and a Ag/AgCl reference electrode. The voltage was set to −0.345 V, and the reaction proceeded in an anaerobic chamber overnight until the current reached zero.

The three other phenazines underwent only chemical reduction. For 1-hydroxyphenazine, 500 μM stocks were diluted in 1× MOPS buffer with pH 7-buffered DTT as the reducing agent. Five hundred micromolar stocks of phenazine-1-carboxamide and phenazine-1-carboxylic acid were diluted in 1× MOPS buffer with 5 mM TCEP.

Hyperspectral and Fluorescence Lifetime Imaging on Zeiss LSM-880. To characterize the emission spectra and fluorescence lifetime of NADH, FAD, pyoverdine, reduced pyocyanin, and reduced 1-hydroxyphenazine, pure solutions were transferred to a clean slide. Reduced pyocyanin and 1-hydroxyphenazine were prepared in a Coy anaerobic chamber and sealed with iSpacers to avoid oxygen exposure (https://www.sunjinlab.com/).

The pure fluorophore solutions were imaged on an inverted Zeiss LSM-880 instrument with an ISS Spartan3 FLIMbox, BH HPM-100-40-Hybrid detector, and a Spectra Physics MaiTai titanium-sapphire laser. The fluorophores were excited with two-photon excitation at 740 nm and laser power ranging from 1 to 10 mW. For hyperspectral imaging, emission ranging from 410 to 695 nm was collected with 9 nm step resolution over 32 channels. One frame was collected per sample with a pixel dwell time of 4 μs. The spectra were analyzed on Zeiss Zen software, and .lsm files were exported for downstream steps. After the spectra were collected, the fluorescence lifetime of the same sample was obtained by switching the light path to the FLIMbox detectors. The sample was excited with the same wavelength and laser power as those in the spectral images. The emission was filtered with a 495 nm LP dichroic and Semrock 442/46 nm BrightLine single-band bandpass filter (CFW-BP01-Clin-25). The fluorescence lifetime data was acquired using SimFCS v4-20200515. To obtain enough fluorescence lifetime signal for the downstream analysis, 10−30 frames were collected per sample, with a frame size of 256 × 256 pixels and pixel dwell time of 32 μs.

Z-stack Fluorescence Lifetime of Biofilms on the DIVER Microscope. Intact WT *P. aeruginosa* PA14 biofilms were grown in ASM for 3 days and prepared for Z-stack imaging by adding a large coverslip on top of the surface of the biofilm and then imaged with a 0.8 Olympus LUMPLFLN 40XW Objective. Z-stacks were obtained on a custom-made microscope at the Laboratory for Fluorescence Dynamics, the DIVER (Deep Imaging Via Enhanced Recovery).[19,20] The DIVER is a Nikon Eclipse TE2000-U microscope equipped with a wide-area 18 × 18 mm photomultiplier tube (PMT) (Hamamatsu R7600P-300) which enhances photon collection. Samples were excited with 2-photon excitation at 740 nm using a Tsunami Spectra-Physics Ti:sapphire laser (80 MHz). The emission was filtered with a Schott BG-39 filter and NADH-targeted optical band-pass filter (400−500 nm). Fluorescence lifetime data was collected with SimFCS v4 software. Z-stacks were automatically acquired every 100 μm from the surface of the biofilm to 1 mm deep, which was the maximum depth at which the FLIM-phasor signal was distinct from uninoculated media for WT cultures. The laser power was increased with an exponential function for deeper sample imaging, with the power ranging from 1 to 58 mW.

Fluorescence Lifetime Analysis and Visualization. The pixels in the fluorescent images were median-filtered prior to downstream intensity and lifetime analyses. SimFCS v4-20200515 software was used to calculate phasor *G* and *S* values for each pixel.[36] Plotting and statistical analyses were performed in python and R (https://github.com/tgallagh/PseudomonasFLIM). Specifically, color-mapped FLIM figures were created by assigning *G* and *S* coordinates to approximately 13,000 to 20,000 2-D bins. Spline interpolation across three base colors (orange, green, and blue) generated a palette of 600 colors, which were assigned to sorted bins and the corresponding pixels.

https://doi.org/10.1021/acsinfecdis.4c00489
ACS Infect. Dis. 2025, 11, 543−549

■ ASSOCIATED CONTENT

Supporting Information

The Supporting Information is available free of charge at https://pubs.acs.org/doi/10.1021/acsinfecdis.4c00489.

Fluorescent emission spectra of all fluorophores, including fluorophores with emission spectra outside of the FLIM range; Fluorescent spectra and lifetime signal for chemically and electrochemically reduced pyocyanin; Fluorescent intensity signal at the surface vs bottom of the biofilm and similar lifetime signal for different frame counts; FLIM distributions for *P. aeruginosa* biofilms compared to uninoculated media FLIM-phasor signal for different bacteria; Comparison of FLIM signal for biofilms with and without a coverslip; Pairwise *t* test results for phasor coordinates for different biofilm depths; Pairwise *t* test results for phasor coordinates for cross-feeding conditions (PDF)

■ AUTHOR INFORMATION

Corresponding Author

Katrine Whiteson − *University of California Irvine, Department of Molecular Biology and Biochemistry, Irvine, California 92697-2525, United States;* orcid.org/0000-0002-5423-6014; Email: katrine@uci.edu

Authors

Tara Gallagher − *University of California Irvine, Department of Molecular Biology and Biochemistry, Irvine, California 92697-2525, United States*

Simon Leemans − *University of California Irvine, Department of Biomedical Engineering, Irvine, California 92697-2715, United States*

Alexander S. Dvornikov − *University of California Irvine, Department of Biomedical Engineering, Irvine, California 92697-2715, United States*

Kumar Perinbam − *University of California Irvine, Department of Molecular Biology and Biochemistry, Irvine, California 92697-2525, United States; Dayananda Sagar University, School of Basic and Applied Sciences, Ramanagara, Karnataka 562112, India*

Joshua Fong − *University of California Irvine, Department of Molecular Biology and Biochemistry, Irvine, California 92697-2525, United States*

Christina Kim − *University of California Irvine, Department of Molecular Biology and Biochemistry, Irvine, California 92697-2525, United States*

Joseph Kapcia − *University of California Irvine, Department of Molecular Biology and Biochemistry, Irvine, California 92697-2525, United States*

Miki Kagawa − *University of California Irvine, Department of Molecular Biology and Biochemistry, Irvine, California 92697-2525, United States*

Adam Grosvirt-Dramen − *University of California Irvine, Department of Chemical and Biomolecular Engineering, 6000 Interdisciplinary Science & Engineering Building (ISEB), Irvine, California 92617-2580, United States*

Allon I. Hochbaum − *University of California Irvine, Department of Materials Science and Engineering, Irvine, California 92697-2585, United States; University of California Irvine, Department of Chemistry, Irvine, California 92697-2025, United States; University of California Irvine, Department of Chemical and Biomolecular Engineering, 6000 Interdisciplinary Science & Engineering Building (ISEB), Irvine, California 92617-2580, United States; University of California Irvine, Department of Molecular Biology and Biochemistry, Irvine, California 92697-2525, United States;* orcid.org/0000-0002-5377-8065

Michelle A. Digman − *University of California Irvine, Department of Biomedical Engineering, Irvine, California 92697-2715, United States;* orcid.org/0000-0003-4611-7100

Enrico Gratton − *University of California Irvine, Department of Biomedical Engineering, Irvine, California 92697-2715, United States*

Albert Siryaporn − *University of California Irvine, Department of Physics and Astronomy, Irvine, California 92697-4575, United States*

Complete contact information is available at: https://pubs.acs.org/10.1021/acsinfecdis.4c00489

Author Contributions

#T.G. and S.L. contributed equally.

Funding

This work was supported by the UC Irvine Center for Complex Biological Systems Opportunity Award, funded by the NIH-NIGMS (National Institute of General Medical Sciences) P50-GM076516 grant NIH NHLBI (R01 HL136647−04) and by start-up funds for the Whiteson lab in the UC Irvine Molecular Biology and Biochemistry Department. T.G. and S.L. were supported through National Science Foundation's Integrative Graduate Education and Research Traineeship (IGERT) program (grant DGE-1144901). This research was also partially supported by the National Science Foundation Materials Research Science and Engineering Center program through the UC Irvine Center for Complex and Active Materials (DMR-2011967).

Notes

The authors declare no competing financial interest.

■ ABBREVIATIONS

ASM, artificial sputum medium; CPX, coproporphyrin; DTT, dithiothreitol; FLIM, fluorescence lifetime imaging microscopy; LDH, lactate dehydrogenase; OHPhz, 1-hydroxyphenazine; OLS, oxidized lipid signal; PCA, phenazine-1-carboxylic acid; PCN, phenazine-1-carboxamide; PVD, pyoverdine; PYO, pyocyanin; suc, succinate; sup, supernatant; TCEP, tris(2-carboxyethyl)phosphine; Δ*phz*, *P. aeruginosa* PA14 Δ*phzA1-G1*/Δ*phzA2-G2*

■ REFERENCES

(1) Cowley, E. S.; Kopf, S. H.; LaRiviere, A.; Ziebis, W.; Newman, D. K. Pediatric cystic fibrosis sputum can be chemically dynamic, anoxic, and extremely reduced due to hydrogen sulfide formation. *mBio* **2015**, *6* (4), No. e00767-15.

(2) Worlitzsch, D.; Tarran, R.; Ulrich, M.; Schwab, U.; Cekici, A.; Meyer, K. C.; et al. Effects of reduced mucus oxygen concentration in airway Pseudomonas infections of cystic fibrosis patients. *J. Clin. Invest.* **2002**, *109* (3), 317−325.

(3) Martin, L. W.; Gray, A. R.; Brockway, B.; Lamont, I. L. Pseudomonas aeruginosa is oxygen-deprived during infection in cystic fibrosis lungs, reducing the effectiveness of antibiotics. *FEMS Microbiology Letters* **2023**, *370*, fnad076.

(4) Kolpen, M.; Hansen, C. R.; Bjarnsholt, T.; Moser, C.; Christensen, L. D.; van Gennip, M.; et al. Polymorphonuclear

leucocytes consume oxygen in sputum from chronic Pseudomonas aeruginosa pneumonia in cystic fibrosis. *Thorax* **2010**, *65* (1), 57−62.
(5) Line, L.; Alhede, M.; Kolpen, M.; Kühl, M.; Ciofu, O.; Bjarnsholt, T.; et al. Physiological levels of nitrate support anoxic growth by denitrification of Pseudomonas aeruginosa at growth rates reported in cystic fibrosis lungs and sputum. *Frontiers in Microbiology* **2014**, *5*, 544.
(6) Palmer, K. L.; Brown, S. A.; Whiteley, M. Membrane-Bound Nitrate Reductase Is Required for Anaerobic Growth in Cystic Fibrosis Sputum. *J. Bacteriol.* **2007**, *189* (12), 4449−4455.
(7) Price-Whelan, A.; Dietrich, L. E. P.; Newman, D. K. Rethinking "secondary" metabolism: physiological roles for phenazine antibiotics. *Nat. Chem. Biol.* **2006**, *2* (2), 71−78.
(8) Glasser, N. R.; Kern, S. E.; Newman, D. K. Phenazine redox cycling enhances anaerobic survival in Pseudomonas aeruginosa by facilitating generation of ATP and a proton-motive force. *Mol. Microbiol.* **2014**, *92* (2), 399−412.
(9) Ciemniecki, J. A.; Newman, D. K. The Potential for Redox-Active Metabolites To Enhance or Unlock Anaerobic Survival Metabolisms in Aerobes. *J. Bacteriol.* **2020**, *202* (11), No. e00797-19.
(10) Lau, G. W.; Ran, H.; Kong, F.; Hassett, D. J.; Mavrodi, D. Pseudomonas aeruginosa Pyocyanin Is Critical for Lung Infection in Mice. *Infect. Immun.* **2004**, *72* (7), 4275−4278.
(11) Jiménez Otero, F.; Newman, D. K.; Tender, L. M. Pyocyanin-dependent electrochemical inhibition of Pseudomonas aeruginosa biofilms is synergistic with antibiotic treatment. *mBio* **2023**, *14* (4), No. e0070223.
(12) Pierson, L. S.; Keppenne, V. D.; Wood, D. W. Phenazine antibiotic biosynthesis in Pseudomonas aureofaciens 30−84 is regulated by PhzR in response to cell density. *J. Bacteriol.* **1994**, *176* (13), 3966−3974.
(13) Khan, S. R.; Mavrodi, D. V.; Jog, G. J.; Suga, H.; Thomashow, L. S.; Farrand, S. K. Activation of the phz Operon of Pseudomonas fluorescens 2−79 Requires the LuxR Homolog PhzR, N-(3-OH-Hexanoyl)-l-Homoserine Lactone Produced by the LuxI Homolog PhzI, and a cis-Acting phz Box. *J. Bacteriol.* **2005**, *187* (18), 6517−6527.
(14) Phan, J.; Gallagher, T.; Oliver, A.; England, W. E.; Whiteson, K. Fermentation products in the cystic fibrosis airways induce aggregation and dormancy-associated expression profiles in a CF clinical isolate of Pseudomonas aeruginosa. *FEMS microbiology letters* **2018**, *365* (10), fny082.
(15) Venkataraman, A.; Rosenbaum, M. A.; Werner, J. J.; Winans, S. C.; Angenent, L. T. Metabolite transfer with the fermentation product 2,3-butanediol enhances virulence by Pseudomonas aeruginosa. *ISME Journal* **2014**, *8* (6), 1210−1220.
(16) Saunders, S. H.; Edmund, C. M.; Yates, M. D.; Otero, F. J.; Trammell, S. A.; Stemp, E. D.; et al. Extracellular DNA promotes efficient extracellular electron transfer by pyocyanin in Pseudomonas aeruginosa biofilms. *Cell* **2020**, *182* (4), 919−932.
(17) Hall, S.; McDermott, C.; Anoopkumar-Dukie, S.; McFarland, A. J.; Forbes, A.; Perkins, A. V.; et al. Cellular Effects of Pyocyanin, a Secreted Virulence Factor of Pseudomonas aeruginosa. *Toxins* **2016**, *8* (8), 236.
(18) Sullivan, N. L.; Tzeranis, D. S.; Wang, Y.; So, P. T. C.; Newman, D. Quantifying the Dynamics of Bacterial Secondary Metabolites by Spectral Multiphoton Microscopy. *ACS Chem. Biol.* **2011**, *6* (9), 893−899.
(19) Dvornikov, A.; Malacrida, L.; Gratton, E. The DIVER Microscope for Imaging in Scattering Media. *Methods and Protocols* **2019**, *2* (2), 53.
(20) Leemans, S.; Dvornikov, A.; Gallagher, T.; Gratton, E. AO DIVER: Development of a three-dimensional adaptive optics system to advance the depth limits of multiphoton imaging. *APL Photonics* **2020**, *5* (12), 120801.
(21) Digman, M. A.; Caiolfa, V. R.; Zamai, M.; Gratton, E. The Phasor Approach to Fluorescence Lifetime Imaging Analysis. *Biophys. J.* **2008**, *94* (2), L14−L16.
(22) Vallmitjana, A.; Dvornikov, A.; Torrado, B.; Jameson, D. M.; Ranjit, S.; Gratton, E. Resolution of 4 components in the same pixel in FLIM images using the phasor approach. *Methods and Applications in Fluorescence* **2020**, *8* (3), 035001.
(23) Datta, R.; Heylman, C.; George, S. C.; Gratton, E. Label-free imaging of metabolism and oxidative stress in human induced pluripotent stem cell-derived cardiomyocytes. *Biomedical Optics Express* **2016**, *7* (5), 1690−1701.
(24) Sakhtah, H.; Koyama, L.; Zhang, Y.; Morales, D. K.; Fields, B. L.; Price-Whelan, A.; et al. The Pseudomonas aeruginosa efflux pump MexGHI-OpmD transports a natural phenazine that controls gene expression and biofilm development. *Proc. Natl. Acad. Sci. U.S.A.* **2016**, *113* (25), No. E3538-E3547.
(25) Jameson, D. M.; Thomas, V.; Zhou, D. Time-resolved fluorescence studies on NADH bound to mitochondrial malate dehydrogenase. *Biochimica et Biophysica Acta (BBA) - Protein Structure and Molecular Enzymology* **1989**, *994* (2), 187−190.
(26) Ranjit, S.; Malacrida, L.; Stakic, M.; Gratton, E. Determination of the metabolic index using the fluorescence lifetime of free and bound nicotinamide adenine dinucleotide using the phasor approach. *Journal of Biophotonics* **2019**, *12* (11), No. e201900156.
(27) Neubauer, C.; Kasi, A. S.; Grahl, N.; Sessions, A. L.; Kopf, S. H.; Kato, R.; et al. Refining the Application of Microbial Lipids as Tracers of Staphylococcus aureus Growth Rates in Cystic Fibrosis Sputum. *J. Bacteriol.* **2018**, *200* (24), No. e00365-18.
(28) Kopf, S. H.; Sessions, A. L.; Cowley, E. S.; Reyes, C.; Sambeek, L. V.; Hu, Y.; et al. Trace incorporation of heavy water reveals slow and heterogeneous pathogen growth rates in cystic fibrosis sputum. *Proc. Natl. Acad. Sci. U. S. A.* **2016**, *113* (2), No. E110-E116.
(29) Bhattacharjee, A.; Datta, R.; Gratton, E.; Hochbaum, A. I. Metabolic fingerprinting of bacteria by fluorescence lifetime imaging microscopy. *Sci. Rep.* **2017**, *7* (1), 1−10.
(30) Perinbam, K.; Chacko, J. V.; Kannan, A.; Digman, M. A.; Siryaporn, A. A Shift in Central Metabolism Accompanies Virulence Activation in Pseudomonas aeruginosa. *mBio* **2020**, *11* (2), No. e02730-18.
(31) Parsons, J. F.; Greenhagen, B. T.; Shi, K.; Calabrese, K.; Robinson, H.; Ladner, J. E. Structural and Functional Analysis of the Pyocyanin Biosynthetic Protein PhzM from Pseudomonas aeruginosa. *Biochemistry* **2007**, *46* (7), 1821−1828.
(32) Wang, Y.; Newman, D. K. Redox reactions of phenazine antibiotics with ferric (hydr) oxides and molecular oxygen. *Environ. Sci. Technol.* **2008**, *42* (7), 2380−2386.
(33) Glasser, N. R.; Wang, B. X.; Hoy, J. A.; Newman, D. K. The pyruvate and α-ketoglutarate dehydrogenase complexes of Pseudomonas aeruginosa catalyze pyocyanin and phenazine-1-carboxylic acid reduction via the subunit dihydrolipoamide dehydrogenase. *J. Biol. Chem.* **2017**, *292*, 5593.
(34) Gao, B.; Gallagher, T.; Zhang, Y.; Elbadawi-Sidhu, M.; Lai, Z.; Fiehn, O.; et al. Tracking polymicrobial metabolism in cystic fibrosis airways: Pseudomonas aeruginosa metabolism and physiology are influenced by Rothia mucilaginosa-derived metabolites. *mSphere* **2018**, *3* (2), No. e00151-18.
(35) Torrado, B.; Vallmitjana, A.; Dvornikov, A.; Gratton, E. Simultaneous FLIM, harmonic generation and hyperspectral imaging using a 4-channel detector. *Biophys. J.* **2023**, *122* (3), 280a.
(36) Ranjit, S.; Malacrida, L.; Jameson, D. M.; Gratton, E. Fit-free analysis of fluorescence lifetime imaging data using the phasor approach. *Nat. Protoc.* **2018**, *13* (9), 1979−2004.

https://doi.org/10.1021/acsinfecdis.4c00489
ACS Infect. Dis. 2025, 11, 543−549